Supporting Information

MOFs-Derived Hollow Multi-shell $NiCo_2O_4$ Spheres as High-Performance Cathodes for Alkaline Aqueous Zn Batteries

Jingliang Wang,[ab] Xiaoyu Cheng,[ad] Dechao Chen,*[a] Jiaqi Yu,*[cd] Zailai Xie,[a] Changsheng Cao*[a]

[a] Key Laboratory of Advanced Carbon-Based Functional Materials (Fujian Province University), Fuzhou University, Fuzhou 350016 Fujian, China.

[b] School of Physical Science and Technology, ShanghaiTech University, Shanghai 201210, China.

[c] College of Materials Science and Engineering, Fuzhou University, Fuzhou 350108, China.

[d] State Key Laboratory of Structural Chemistry, and Fujian Provincial Key Laboratory of Materials and Techniques toward Hydrogen Energy, Fujian Institute of Research on the Structure of Matter, Chinese Academy of Sciences, Fuzhou, Fujian, 350002, China.

E-mail addresses: chendechao@fzu.edu.cn (D. Chen), yujiaqi@fjirsm.ac.cn (J. Yu), cscao@fzu.edu.cn (C. Cao)

Additional characterization results

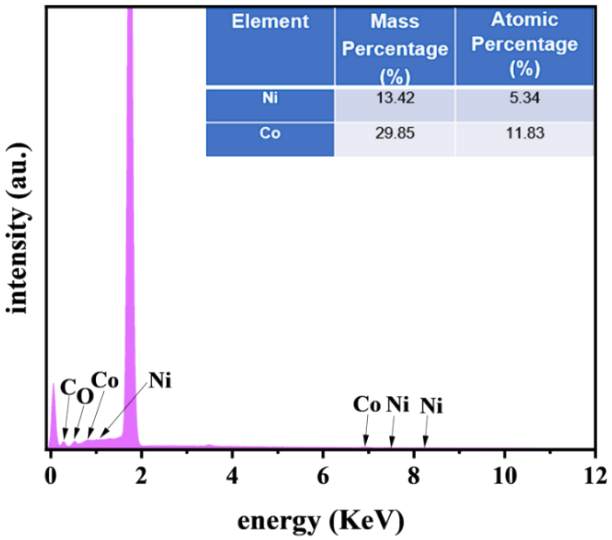

Fig. S1. Atomic percentage of each element in the NiCo-MOF.

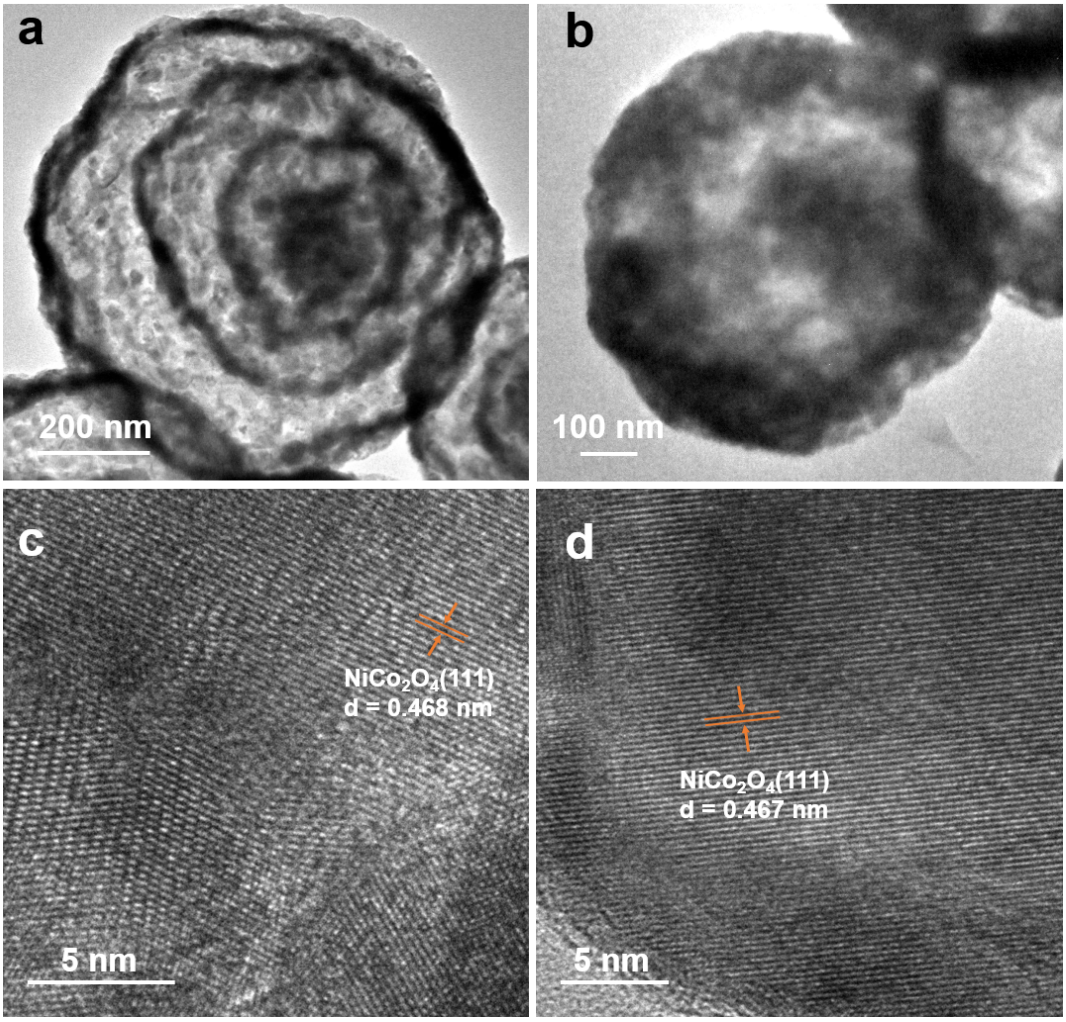

Fig. S2. High-magnification TEM images of (a, c) $NiCo_2O_4$-HMSs and (b, d) $NiCo_2O_4$-HSs.

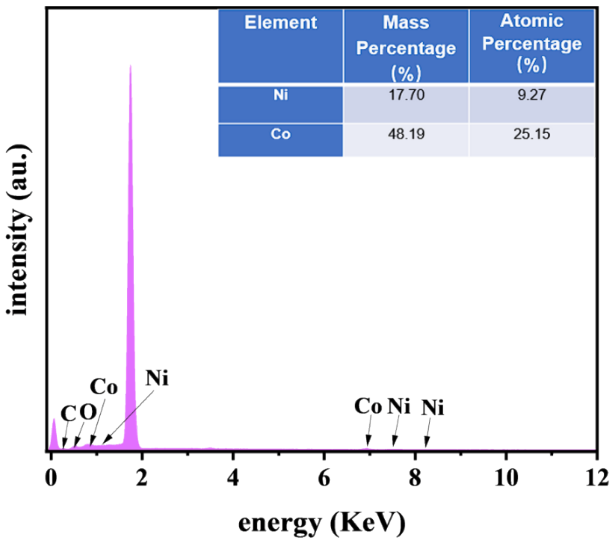

Fig. S3. Atomic percentage of each element in the $NiCo_2O_4$-HMSs.

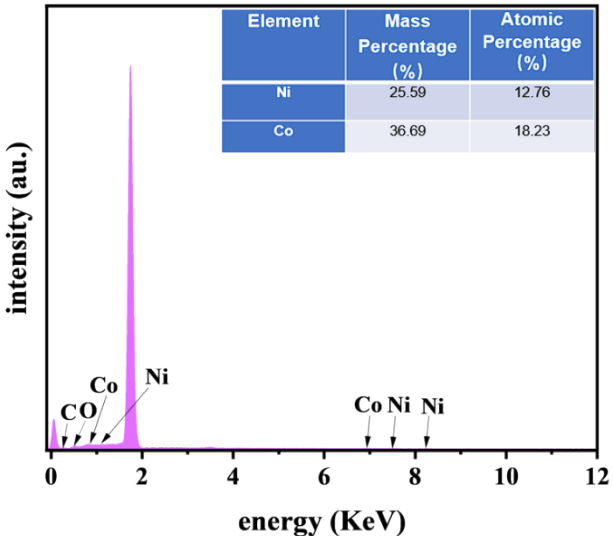

Fig. S4. Atomic percentage of each element in the $NiCo_2O_4$-HSs.

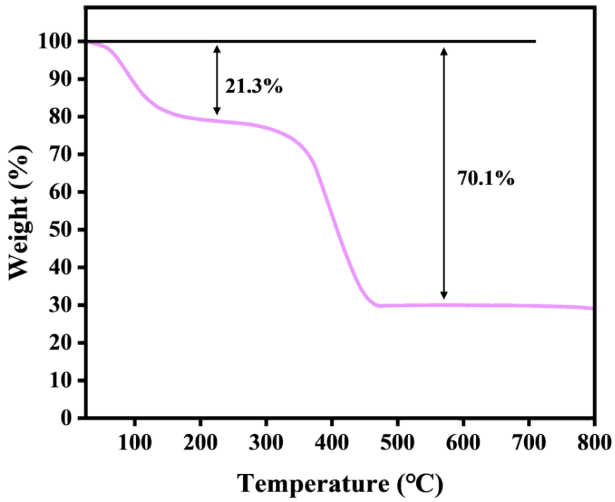

Fig. S5. Thermogravimetric curve of NiCo-MOF.

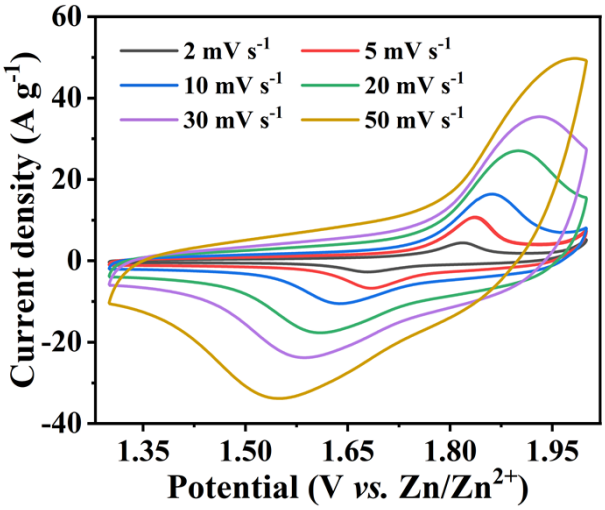

Fig. S6. CV curves of the $NiCo_2O_4$-HSs//Zn battery at different scan rates.

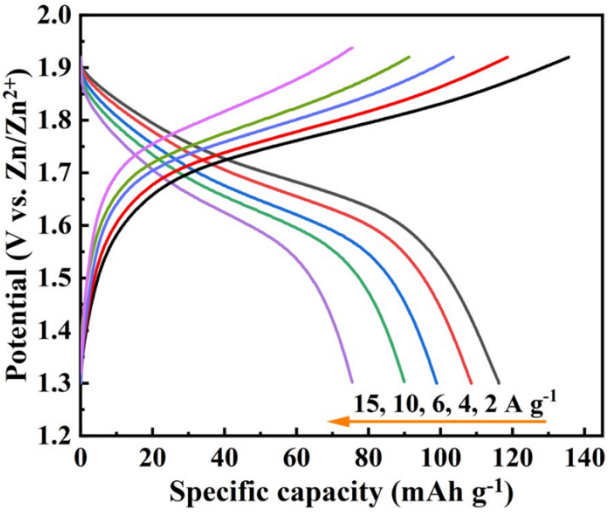

Fig. S7. GCD curves of the $NiCo_2O_4$-HSs//Zn battery.

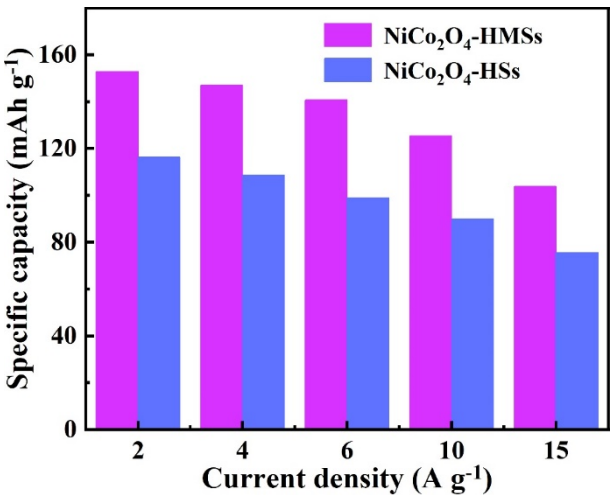

Fig. S8. Comparison of the specific capacities of the $NiCo_2O_4$-HMSs//Zn and $NiCo_2O_4$-HSs//Zn batteries.

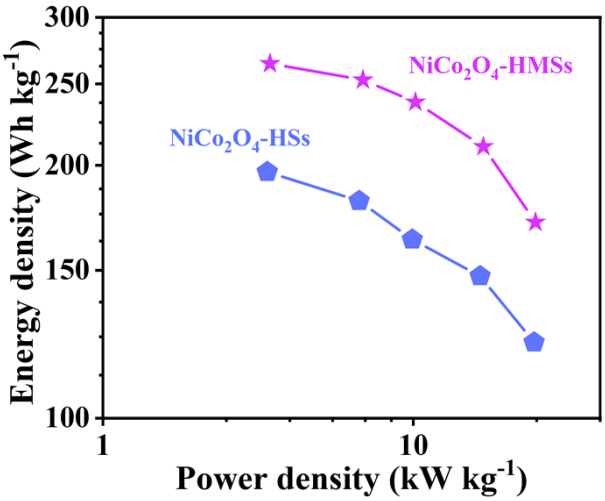

Fig. S9. Ragone plots comparing the energy and power densities of the $NiCo_2O_4$-HMSs//Zn and $NiCo_2O_4$-HSs//Zn batteries.

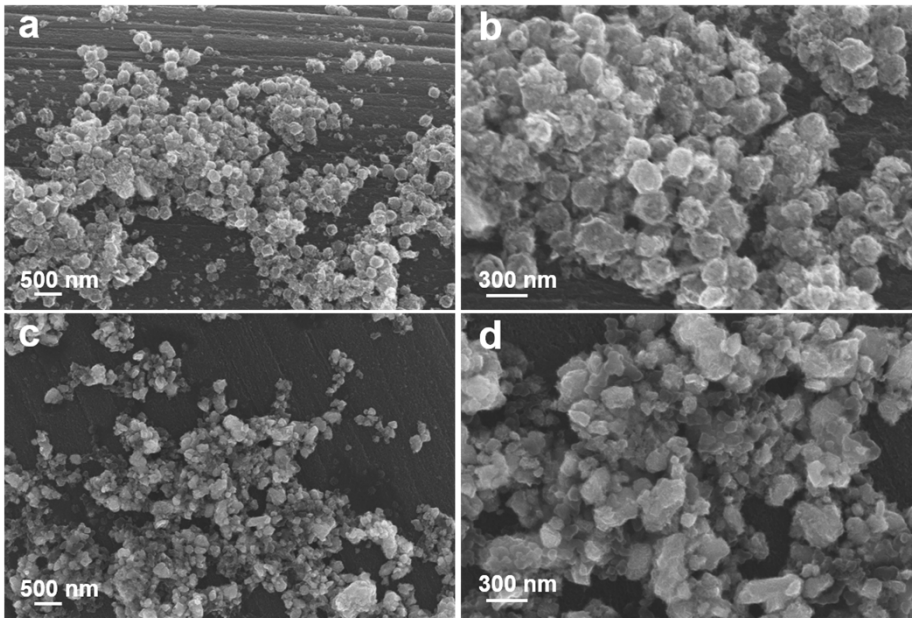

Fig. S10. SEM images of (a, b) $NiCo_2O_4$-HMSs and (c, d) $NiCo_2O_4$-HSs after cycling.

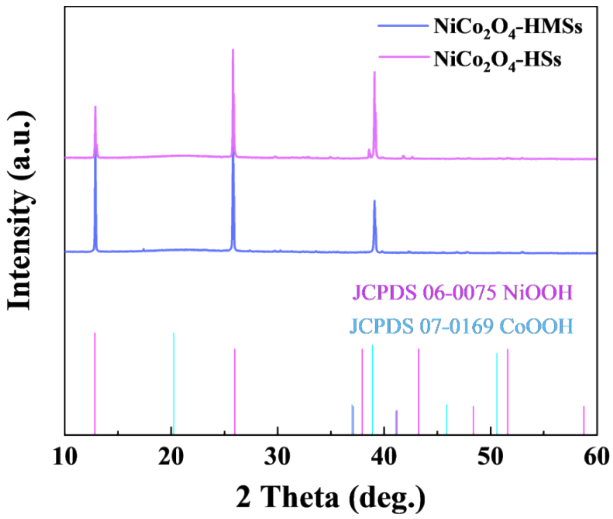

Fig. S11. XRD patterns of the cycled cathodes.

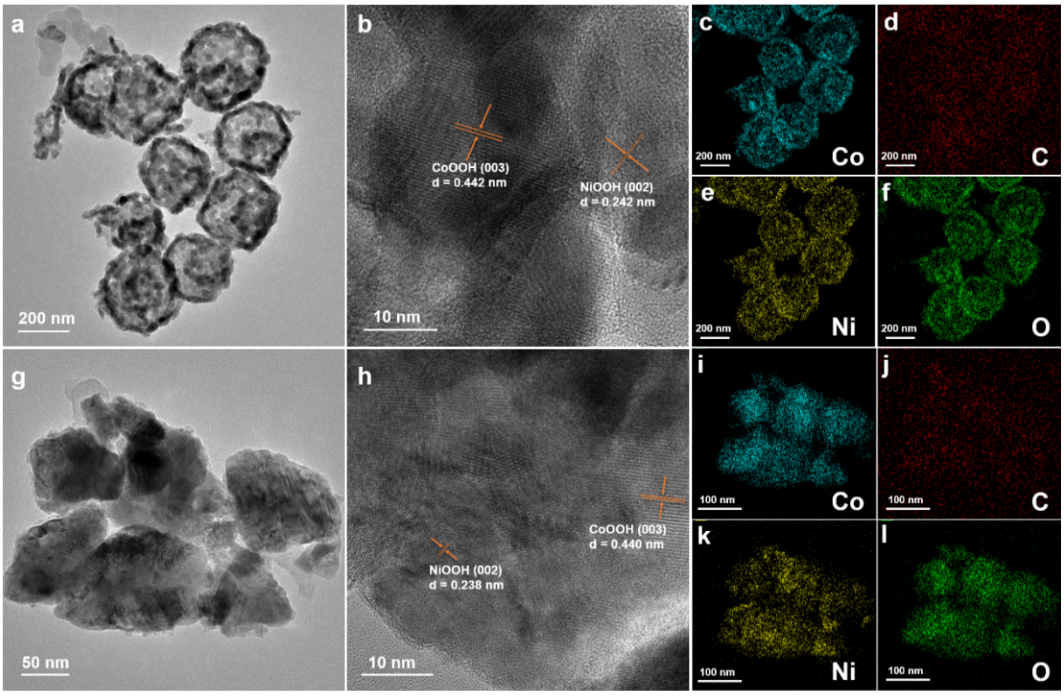

Fig. S12. (a) TEM, (b) HRTEM, and (c-f) EDS elemental mapping images of $NiCo_2O_4$-HMSs after cycling. (g) TEM, (h) HRTEM, and (i-l) EDS elemental mapping images of $NiCo_2O_4$-HSs after cycling.

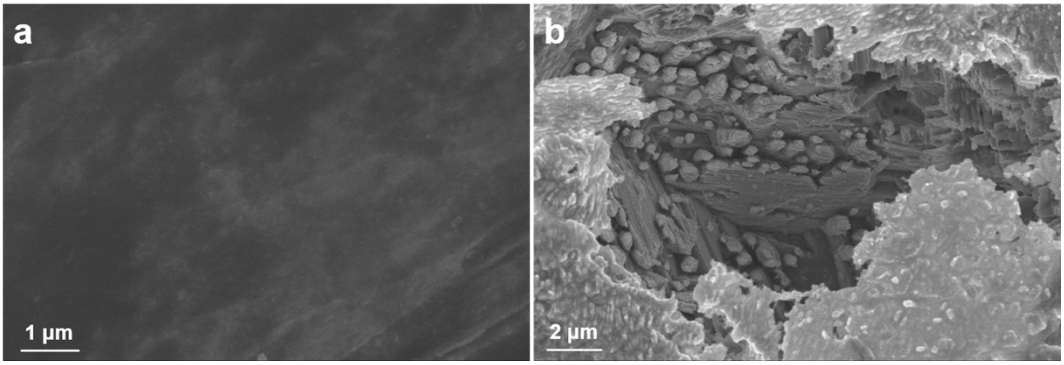

Fig. S13. SEM images of the Zn anode before (a) and after (b) cycling.

Table S1. Comparison of the specific capacity and cycle stability with other previously reported works.

Energy storage device	Specific capacity	Cycle stability	Refs.
$NiCo_2O_4$-HMSs//Zn battery	**152.8 mAh g^{-1} at 2 A g^{-1}**	**86.5% after 500 cycles**	**This Work**
G-NCGs//Zn battery	113.8 mAh g^{-1} at 0.5 A g^{-1}	90% after 650 cycles	[1]
Ni-BTC-5// Zn battery	210.6 mAh g^{-1} at 1 A g^{-1}	80.2% after 3000 cycles	[2]
CH@NC-LDH@NT//Zn battery	55.6 mAh g^{-1} at 1.1 A g^{-1}	71% after 800 cycles	[3]
$NiCo_2O_4$//Zn battery	211.7 mAh g^{-1} at 2 A g^{-1}	63.2% after 1000 cycles	[4]
NiSe//Zn-KFC battery	215.0 mAh g^{-1} at 4.2 A g^{-1}	63.4% after 1300 cycles	[5]

References

[1] X. Zhang, J. He, L. Zhou, H. Zhang, Q. Wang, B. Huang, X. Lu, Y. Tong, C. Wang, *Adv Funct. Mater.*, 2021, **31**, 2100443.

[2] F. Zhang, J. Ma, Z. Wu, Y. Hu, X. Cao, H. Yao, *Inorg. Chem.*, 2025, **64**, 9294−9302.

[3] Y. Wang, X. Hong, Y. Guo, Y. Zhao, X. Liao, X. Liu, Q. Li, L. He, L. Mai, *Small*, 2020, **16**, 2000293.

[4] W. Shang, W. Yu, P. Tan, B. Chen, H. Xu, M. Ni, *J. Power Sources*, 2020, **421**, 6−13.

[5] Y. Huang, M. Li, S. Chen, P. Sun, X. Lv, B. Li, L. Fang, X. Sun, *Appl. Surf. Sci.*, 2021, **562**,150222.